

# Numerical analysis of a new magnetic frequency tripler with series-connected reactors

メタデータ	言語: eng 出版者: 公開日: 2017-10-03 キーワード (Ja): キーワード (En): 作成者: メールアドレス: 所属:
URL	<a href="http://hdl.handle.net/2297/48350">http://hdl.handle.net/2297/48350</a>

NUMERICAL ANALYSIS OF A NEW MAGNETIC FREQUENCY TRIPLER WITH SERIES-CONNECTED REACTORS

T. Sudani  
 Kanazawa Institute of Technology  
 Kanazawa, Japan

S. Yamada K. Bessho  
 Kanazawa University  
 Kanazawa, Japan

ABSTRACT

The authors propose a new magnetic frequency tripler with series-connected reactors, and present a numerical analysis of the tripler. In the analysis,  $\phi$ -i characteristic of saturable reactor is approximated by fifth-order polynomial, and nonlinear ordinary differential equations for flux linkage are derived from an equivalent circuit. The nonlinear simultaneous equations, which are obtained by using the method of Harmonic Balance, are solved by an improved Newton's method. The improved numerical method enables to determine optimum gap length and coil turns of the reactors. Experimental results, which are obtained by using the reactors with the numerically determined gap length and coil turns, show a constant voltage characteristic up to a certain load and a drooping characteristic above that load.

INTRODUCTION

In general 3-phase magnetic frequency triplers are utilized as triple frequency power sources for supplying induction heating loads<sup>1</sup>, and single-phase triplers are utilized as small-sized power sources for supplying luminous sources. Regarding the single-phase tripler, the authors previously reported a magnetic frequency tripler with bridge-connected reactor circuit, and reported some experiments and considerations; but, the design of this tripler was largely empirical.<sup>2,3</sup> The authors afterwards proposed a tripler with series-connected reactors which was equivalent to the tripler with bridge-connected reactor circuit and was simple in structure. We also reported numerical analysis; but, the numerical results were insufficient to be used as a basis for the design method.<sup>4-6</sup>

The purpose of this paper is to obtain numerical results, which can be used as a basis for the computer-aided design, by analyzing an equivalent circuit containing conductance, ohmic resistance and leakage reactance. This paper describes the numerical analysis and the experimental results of the tripler composed of the reactors with numerically determined gap length and coil turns.

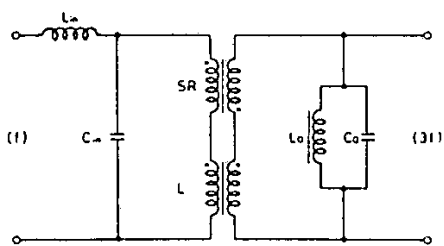


Fig. 1 A magnetic frequency tripler

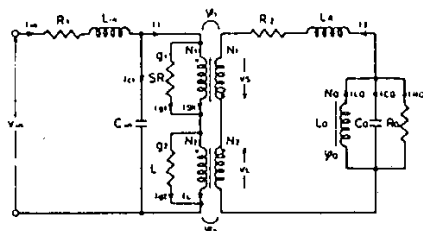


Fig. 2 Equivalent circuit

Manuscript received June 6, 1979.

CIRCUIT EQUATION

As shown in Fig.1, this tripler is composed of an input filter network with a linear reactor  $L_{in}$ , a capacitor  $C_{in}$  and the basic tripler circuit. The basic tripler circuit consists of a saturable reactor SR, a linear reactor  $L$  and a ferro-resonance circuit  $L_0$ - $C_0$ . Figure 2 shows an equivalent circuit used for the numerical analysis. In this figure,  $R_1$  and  $R_2$  are the ohmic resistance,  $G_1$  and  $G_2$  the conductance and  $R_0$  the equivalent resistance of the load resistance  $R_L$  and the conductance  $G_0$  in parallel; furthermore,  $L_r$  is the leakage reactance. Referring to Fig. 2, the following nonlinear ordinary differential equations for the instantaneous value of the core flux are obtained:

$$CoNo \frac{d^2 \phi_0}{dt^2} + \frac{No}{R_0} \frac{d\phi_0}{dt} + \frac{1}{No} h(\phi_0) + \frac{G_1 N_1}{2} \frac{d\phi_1}{dt} + \frac{1}{2N_1} f(\phi_1) - \frac{G_2 N_2}{2} \frac{d\phi_2}{dt} - \frac{\alpha_2}{2N_2} \phi_2 = 0 \quad (1)$$

$$No \frac{d\phi_0}{dt} - \frac{Lr G_1 N_1}{2} \frac{d^2 \phi_1}{dt^2} - k_1 \frac{d\phi_1}{dt} - \frac{R_1}{2N_1} f(\phi_1) - \frac{Lr}{2N_1} f'(\phi_1) + \frac{Lr G_2 N_2}{2} \frac{d^2 \phi_2}{dt^2} + k_2 \frac{d\phi_2}{dt} + \frac{R_2}{2N_2} g(\phi_2) = 0 \quad (2)$$

$$LinCinN_1 \frac{d^3 \phi_1}{dt^3} + k_3 \frac{d^2 \phi_1}{dt^2} + k_4 \frac{d\phi_1}{dt} + \frac{R_1}{2N_1} f'(\phi_1) + LinCinN_2 \frac{d^3 \phi_2}{dt^3} + k_5 \frac{d^2 \phi_2}{dt^2} + k_6 \frac{d\phi_2}{dt} + \frac{R_1}{2N_2} g(\phi_2) + \sqrt{2} V_{in} \sin \omega t = 0 \quad (3)$$

where

$$f(\phi_1) = \alpha_1 \phi_1 + \beta_1 \phi_1^3 + \gamma_1 \phi_1^5$$

$$g(\phi_2) = \alpha_2 \phi_2$$

$$h(\phi_0) = \alpha_0 \phi_0 + \beta_0 \phi_0^3 + \gamma_0 \phi_0^5$$

$$k_1 = N_1 + \frac{R_1 G_1 N_1}{2} \quad k_2 = N_2 + \frac{R_2 G_2 N_2}{2} + \frac{\alpha_2 Lr}{2N_2}$$

$$k_3 = R_1 CinN_1 + \frac{LinG_1 N_1}{2} \quad k_4 = N_1 + \frac{R_1 G_1 N_1}{2}$$

$$k_5 = R_1 CinN_2 + \frac{LinG_2 N_2}{2} \quad k_6 = N_2 + \frac{R_2 G_2 N_2}{2} + \frac{\alpha_2 Lin}{2}$$

In the above-mentioned equations, the  $\phi$ -i characteristics of saturable reactors are approximated by fifth-order polynomials.

Table 1. Coefficients of polynomial

	SR		Lo	
	SR <sub>1</sub> = 240 turn	SR <sub>2</sub> = 320 turn	Lo <sub>1</sub> = 200 turn	Lo <sub>2</sub> = 250 turn
$\alpha$	0.59613E 06	0.56027E 06	0.15520E 07	0.15466E 07
$\beta$	-0.27672E 13	-0.25672E 13	-0.31287E 13	-0.31288E 13
$\gamma$	0.30667E 19	0.28405E 19	0.33631E 19	0.33671E 19

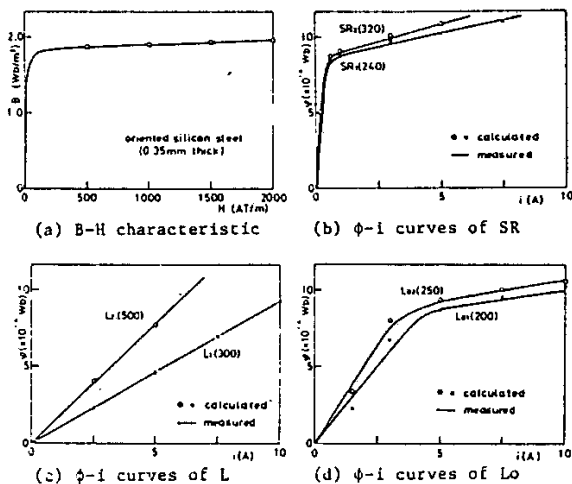


Fig. 3 Magnetizing characteristics. Number in parentheses refer to the number of turns on the reactors.

NUMERICAL ANALYSIS

In the numerical analysis, it is necessary to determine the coefficients  $\alpha$ ,  $\beta$  and  $\gamma$  of the polynomial. Figure 3(a) shows a measured B-H characteristic of the wound core. The  $\phi$ -i characteristic is obtained from the measured B-H characteristic shown in Fig. 3(a). The coefficients of the polynomial are determined by solving simultaneous equations, which are derived by substituting the values of suitably chosen three points on the  $\phi$ -i characteristics into the fifth order polynomial. Table 1 shows calculated results of the coefficients of the fifth-order polynomial. Figure 3(b), (c), (d) show the comparison between the measured curves and the approximated curves of the SR, the L and the Lo respectively.

The aforementioned nonlinear ordinary differential equations are transformed into nonlinear simultaneous equations by using the method of Harmonic Balance<sup>7</sup>. The nonlinear simultaneous equations for the unknown coefficients of the fundamental and third-harmonic core flux are solved by Newton's method. In Newton's method, the authors beforehand derive approximated equations which are obtained by eliminating the high order terms of the nonlinear simultaneous equations. Initial values are solved by the approximated equations, and the iteration is done by using the initial values. By the improved Newton's method, the number of iterations decreases; furthermore, quantitative results are obtained. When Newton's method converges, the steady state performance is calculated by the equations in which the instantaneous values of the core flux are transformed into the effective values. Figure 4 shows a flow chart for the entire analysis.

NUMERICAL RESULTS

Let us first consider the basic circuit of the tripler without an input filter. Regarding load charac-

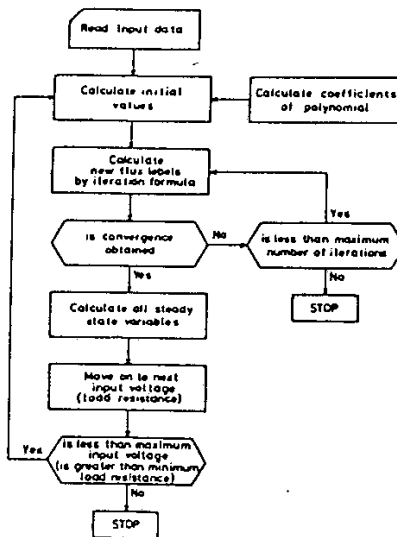


Fig. 4 Computational flow chart

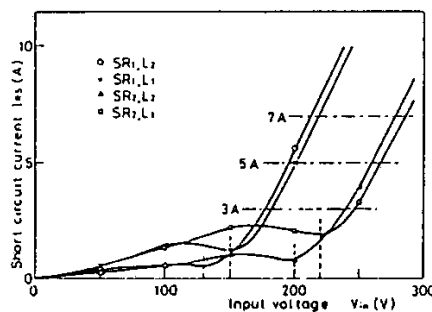


Fig. 5 Short circuit current characteristics

teristics, the maximum load current  $I_{Lmax}$  and the average output power  $P_o$  are important for the optimum design. As  $I_{Lmax}$  is always less than the short circuit current  $I_{sc}$  and the value of  $I_{sc}$  is considered as a rough guess of  $I_{Lmax}$ , we calculate the value of  $I_{sc}$  for various conditions. The curves of the short circuit current for several values of turns of the SR and the L are shown in Fig.5. From Fig.5 it is seen that the short circuit current taken a minimum value and increases in the range exceeding the minimum point.

Next, we analyze load characteristics for various gap length and number of turns of the SR and the L at the input voltages where the values of short circuit current are same. The main calculated results are as follows.

- 1) The arrangement of the SR<sub>2</sub> and the L<sub>1</sub> (low inductance) is best as regards to the maximum load current, efficiency and output power.
- 2) The regulation of the output voltage and the power factor are good, when the inductance of the linear reactor is relatively high such as the L<sub>2</sub>.
- 3) The arrangement of the SR<sub>2</sub> and the L<sub>2</sub> is good as regards to the fundamental component distortion of the output voltage.

These results can be explained by the following reasons: the reason why the value of maximum load current increases is that the electromagnetic energy increases because of the large gap length and low in-

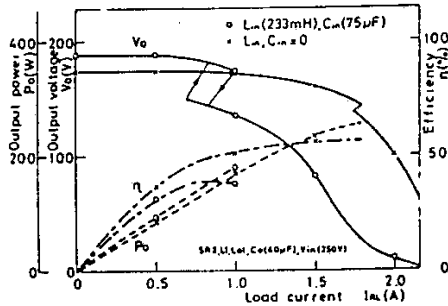


Fig. 6 Load characteristics

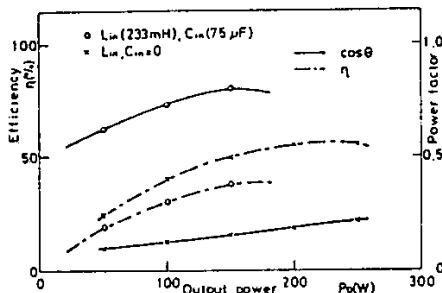


Fig. 7 Efficiency and power factor versus output power

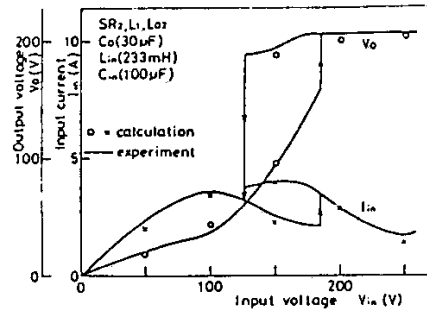


Fig. 8 Voltage characteristics

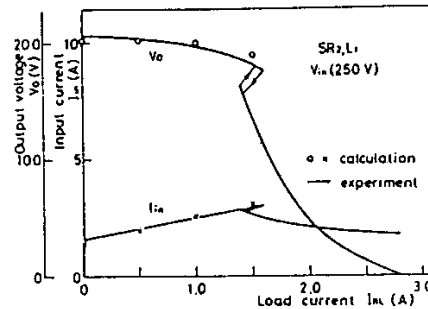


Fig. 9 Load characteristics

ductance of the linear reactor, and the reason why the power factor is high and the fundamental component distortion is low are that the input current and the third-harmonic component of input current decrease because of the high inductance.

As it is desirable that the efficiency and the output power are high, the calculation of the load characteristics is performed with the arrangement of the  $SR_1$  (number of turns of 320) and the  $L_1$  (number of turns of 300 and gap length of 4 mm). Figure 6 shows the load characteristics both with and without an input filter. From Fig. 6 it is clear that the circuit without an input filter is better as regards to  $I_{Lmax}$  and  $P_{omax}$  but the addition of an input filter is better as regards to the regulation of the output voltage. The curves of Fig. 7, which are the calculated by the load characteristics of Fig. 6, are the variation of efficiency and input power factor with the output power. Figure 7 shows that the power factor is improved by the configuration of the tripler with an input filter. It seems therefore that this tripler is practically useful.

EXPERIMENT

The numerically determined gap length of the cores and the arrangement of the  $SR_2$  and the  $L_1$  of the tripler with series-connected reactors are used in the experiment. Figure 8 shows the comparison between the calculation and the experiment of the voltage characteristics. From Fig. 8 it is clear that the regulation of the output voltage is good, and the input current takes a minimum point at the input voltage  $V_{in} = 250$  V.

As the power factor has a maximum value at the minimum point of the input current, the experiment on the load characteristic is performed at  $V_{in} = 250$  V. Figure 9 shows the curves of the load characteristic. In this figure the maximum output power is 290 W, the maximum efficiency  $\eta_{max}$  is about 60% and the maximum power factor  $\cos\theta_{max}$  is 0.83. From Fig. 9 it is seen that the tripler with series-connected reactors has the good regulation and the drooping characteristics on an overload condition. The above-mentioned experimental results are in agreement with the calculated results.

CONCLUSION

This paper has presented a numerical analysis and comparison between the results of analysis and the experiment of the proposed magnetic frequency tripler with series-connected reactors. The main results are as follows.

- 1) It is necessary to take into account the ohmic resistance, the conductance and the leakage reactance in order to obtain quantitative results.
- 2) In Newton's method, it is effective to determine initial values by solving approximated equations of the nonlinear simultaneous equations.
- 3) Optimum gap length and number of turns of the reactors, of which the tripler is composed, can be determined by numerical analysis.
- 4) Experimental results of the load characteristic shows the constant voltage and drooping characteristic; moreover, the results agree with the analytical results.

These results can be used as a basis for the computer-aided design of triplers. In the near future, we hope to establish the method of the optimum computer-aided design by extending the analysis to include optimum core dimension.

REFERENCES

1. J. D. Lavers and P. P. Biringer, IEEE Trans. Magn., Vol. MAG-14, 993 (1978).
2. K. Bessho, S. Yamada, T. Sudani and Y. Kanamaru, IEEE Trans. Magn., Vol. MAG-12, 829 (1976).
3. K. Bessho, S. Yamada and F. Matsumura, IEEE Trans. Magn., Vol. MAG-13, 1217 (1977).
4. T. Sudani, M. Tomino, T. Tsushima and K. Bessho, Convention Record IEE Japan, 540 (1978).
5. T. Sudani and K. Bessho, Memoirs of Kanazawa Institute of Technology, Vol. A-10, 45 (1978).
6. T. Sudani, S. Yamada and K. Bessho, Papers of Technical Meeting on Applied Magnetics, IEE Japan AM-78-42 (1978).
7. C. Hayashi, Nonlinear Oscillation in Physical Systems, New York: McGraw-Hill, 1964.